ORIGINAL ARTICLE

SLIT3 promotes myogenic differentiation as a novel therapeutic factor against muscle loss

Han Jin Cho[1†], Hyeonmok Kim[2†], Young-Sun Lee[1], Sung Ah Moon[1], Jin-Man Kim[1], Hanjun Kim[1], Min Ji Kim[1], Jiyoung Yu[1], Kyunggon Kim[1,3], In-Jeoung Baek[1], Seung Hun Lee[2], Kyong Hoon Ahn[4], Sungsub Kim[5], Jong-Sun Kang[6] & Jung-Min Koh[2*] [iD]

[1]*Asan Institute for Life Sciences, Asan Medical Center, Seoul, South Korea;* [2]*Division of Endocrinology and Metabolism, Asan Medical Center, University of Ulsan College of Medicine, Seoul, South Korea;* [3]*Department of Biomedical Sciences, University of Ulsan College of Medicine, Seoul, South Korea;* [4]*Daewoong Pharmaceutical Co., Ltd, Yongin, South Korea;* [5]*Graduate School of New Drug Discovery and Development, Chungnam National University, Daejeon, South Korea;* [6]*Department of Molecular Cell Biology, Sungkyunkwan University School of Medicine, Suwon, South Korea*

Abstract

Background Sarcopenia and osteoporosis frequently co-occur in the elderly and have common pathophysiological determinants. Slit guidance ligand 3 (SLIT3) has been recently discovered as a novel therapeutic factor against osteoporosis, and a SLIT3 fragment containing the second leucine-rich repeat domain (LRRD2) had a therapeutic efficacy against osteoporosis. However, a role of SLIT3 in the skeletal muscle is unknown.
Methods Skeletal muscle mass, strength, and/or physical activity were evaluated in $Slit3^{-/-}$, ovariectomized, and aged mice, based on the measurements of muscle weight and grip strength, Kondziella's inverted hanging test, and/or wheel-running test. Skeletal muscles were also histologically evaluated by haematoxylin and eosin staining and/or immunofluorescence. The ovariectomized and aged mice were intravenously injected with recombinant SLIT3 LRRD2 for 4 weeks. C2C12 cells were used to know cellular effects of SLIT3, such as in vitro myogenesis, fusion, cell viability, and proliferation, and also used to evaluate its molecular mechanisms by immunocytochemistry, immunoprecipitation, western blotting, real-time PCR, siRNA transfection, and receptor-ligand binding ELISA.
Results $Slit3$-deficient mice exhibited decreased skeletal muscle mass, muscle strength, and physical activity. The relative masses of gastrocnemius and soleus were lower in the $Slit3^{-/-}$ mice (0.580 ± 0.039% and 0.033 ± 0.003%, respectively) than those in the WT littermates (0.622 ± 0.043% and 0.038 ± 0.003%, respectively) (all, $P < 0.05$). Gastrocnemius of $Slit3^{-/-}$ mice showed the reduced number of Type I and Type IIa fibres (all, $P < 0.05$), but not of Type IIb and Type IIx fibres. SLIT3 activated β-catenin signalling by promoting its release from M-cadherin, thereby increasing myogenin expression to stimulate myoblast differentiation. *In vitro* experiments involving ROBO2 expression, knockdown, and interaction with SLIT3 indicated that ROBO2 functions as a SLIT3 receptor to aid myoblast differentiation. SLIT3 LRRD2 dissociated M-cadherin-bound β-catenin and up-regulated myogenin expression to increase myoblast differentiation, in a manner similar to full-length SLIT3. Systemic treatment with SLIT3 LRRD2 increased skeletal muscle mass in both ovariectomized and aged mice (all, $P < 0.05$). The relative masses of gastrocnemius and soleus were higher in the treated aged mice (0.548 ± 0.045% and 0.033 ± 0.005%, respectively) than in the untreated aged mice (0.508 ± 0.016% and 0.028 ± 0.003%, respectively) (all, $P < 0.05$). SLIT3 LRRD2 treatment increased the hanging duration of the aged mice by approximately 1.7-fold ($P < 0.05$).
Conclusions SLIT3 plays a sarcoprotective role by activating β-catenin signalling. SLIT3 LRRD2 can potentially be used as a therapeutic agent against muscle loss.

Keywords Slit3; Robo2; LRRD2; Muscle loss

*Correspondence to: Jung-Min Koh, MD, PhD, Division of Endocrinology and Metabolism, Asan Medical Center, University of Ulsan College of Medicine, 88 Olympic-ro 43-gil, Songpa-gu. Seoul 05505, South Korea. Phone: +82-2-3010-3247, Email: jmkoh@amc.seoul.kr
†Han Jin Cho and Hyeonmok Kim contributed equally to this study.

Introduction

Sarcopenia is characterized by the progressive and general loss of skeletal muscle mass and strength.[1] No anti-sarcopenic drug has been approved, and several that act on known therapeutic targets are currently under development. But most are not effective enough, or the developments have been stopped owing to their adverse effects.[2] Therefore, a new therapeutic target for sarcopenia should be identified.

Slit guidance ligand (SLIT) proteins have been identified as the key regulators of many cellular processes.[3,4] Recently, we identified SLIT3 as a novel anti-osteoporotic factor using a proteomic approach.[5] Bones and muscles are closely related, both anatomically and functionally, and it is known that sarcopenia and osteoporosis have common pathophysiological determinants.[6] Moreover, osteoblasts and myoblasts, which orchestrate bone formation and myogenesis, respectively, have a common origin. Therefore, the same factors may simultaneously play a critical role in osteogenesis and myogenesis, and we hypothesized that SLIT3 also plays a critical role in the skeletal muscle tissue. Further, previous studies have shown that SLIT3 receptors, that is, roundabout (ROBO) family proteins, are expressed in the skeletal muscle,[7,8] and *Slit3*-deficient mice are known to exhibit impaired diaphragmatic muscle development.[9] However, to our knowledge, a role of SLIT3 in the skeletal muscle has not been studied until now. In the present study, we provide experimental evidence—including the results of gene deletion analysis and recombinant SLIT3 fragment treatment—to show that SLIT3 promotes myoblast differentiation and thus can serve as a novel therapeutic target for sarcopenia.

Materials and methods

SLIT3 LRRD2

For bacterial expression, oligonucleotides corresponding to the human *SLIT3* leucine-rich repeat domain 2 (LRRD2) sequence, an *N*-terminal cystatin signal sequence, and a C-terminal FLAG tag were synthesized chemically as previously described with minor modifications.[5] For mammalian expression, SLIT3 LRRD2 was produced by transfecting Expi293F cells (Life Technologies, Carlsbad, CA, USA) with the expression construct, according to the manufacturer's instructions. For further details, refer to the *Supporting information*.

Animals

Animal experimental procedures were approved by the Institutional Animal Care and Use Committee of the Asan Institute for Life Sciences (No. 2015-12-073 and No. 2016-12-035). Cryopreserved *Slit3*[tm1.1Dor]/Mmmh sperm (030759-MU, Mutant Mouse Regional Resource Center, Columbia, MO) was resuscitated by *in vitro* fertilization with female C57BL/6N mouse (Orient Bio Inc., Seongnam, South Korea).[9] The heterozygotes were crossed to generate *Slit3*^{−/−} mice and their wild-type (WT) littermates. PCR-based genotyping was performed. Female C57BL/6 mice were bilaterally ovariectomized at 8 weeks of age. Once the mice reached 9 weeks of age, they were injected with 10-μg SLIT3 LRRD2 or phosphate-buffered saline (PBS) through the tail vein once a day for 5 days a week for a total of 4 weeks. Male C57BL/6 mice at 18 months of age were also intravenously injected with 5 μg SLIT3 LRRD2 or PBS two times a day for 5 days a week for a total of 4 weeks. Six-month–old male C57BL/6 mice were used as young controls. All mice were provided *ad libitum* access to rodent chow and water and were euthanized by cardiac puncture under anaesthesia. For further details, refer to the *Supporting information*.

Cell culture

C2C12 cells, HEK293 cells, HepG2, MCF-7, and MC3T3-E1 were purchased from the American Type Culture Collection (ATCC, Rockville, MD, USA). For further details, refer to the *Supporting information*.

Body composition and relative muscle mass

Body composition was measured using Dual-energy X-ray absorptiometry (Lunar PIXImus, General Electric, Fitchburg, WI, USA). Body composition was expressed as the lean mass and the percentage of fat mass. At the time of euthanization, the gastrocnemius (GC), tibialis anterior (TA), extensor digitorum longus (EDL), and soleus (SOL) muscles were isolated, weighed, and fixed with 4% paraformaldehyde. Relative muscle mass was calculated as follows: relative muscle mass (%) = 100 × muscle weight ÷ body weight.[10]

Measurement of muscle strength and physical activity

Muscle strength was measured using Kondziella's inverted screen test.[11] Briefly, the mice were placed on a wire mesh

screen, and the screen was inverted. Muscle strength was calculated by measuring the hanging duration. Alternatively, the grip strength of the forelimb or four paws was measured using a digital grip strength meter (Jeungdo Bio & Plant Co., Seoul, South Korea). The mean of the peak force (N) of five trials was calculated. Physical activity was measured using a voluntary wheel-running test. The distance of voluntary running per day was calculated using the running wheel system (Starr Life Sciences Corp, Oakmont, PA, USA). The wheel-running activity of each mouse was monitored for 4 days.

Haematoxylin and eosin staining and immunofluorescence

The muscle tissues (10 μm-thick) were prepared using the CM1860 cryostat (Leica Microsystems, Wetzlar, Germany) and were stained with haematoxylin and eosin (H&E). For performing immunofluorescence (IF), the frozen sections were probed overnight with the primary antibody cocktail solution containing three isoform-specific antibodies (Type I, Type IIa, and Type IIb). For further details, refer to the *Supporting information*.

Immunocytochemistry

C2C12 cells were cultured in DMEM supplemented with 2% horse serum for 2 or 3 days. The cells were fixed, permeabilized, and blocked with 2% bovine serum albumin (BSA) for 1 h. The cells were immunostained with antibodies against MyHC or myogenin, and nuclei were counterstained with DAPI. The number and area of MyHC$^+$ myotubes were quantified in six random high-power fields (100×) per group. Fusion index (%) was calculated as follows: 100 × number of nuclei in MyHC$^+$ myotubes/total number of nuclei in MyHC$^+$ myocytes and myotubes.

Immunoprecipitation and Western blotting

Cytosolic fractions and nuclear extracts were prepared using a NE-PER kit (Pierce, Rockford, IL, USA) according to the manufacturer's instructions. For immunoprecipitation (IP), cells were lysed in a lysis buffer [20-mM Tris (pH 7.5), 150-mM NaCl, 1-mM EDTA, 1% Triton X-100, 2.5-mM sodium pyrophosphate, 1-mM β-glycerophosphate, 1-mM Na_3VO_4, 1-mM NaF, and a protease inhibitor mixture]. Cell lysates were precleared using protein A Sepharose beads (GE Healthcare, Piscataway, NJ, USA) and then incubated with anti-M-cadherin antibody at 4°C for 1 h. Next, protein A Sepharose beads were added to the lysates and incubated at 4°C for 1 h. Western blotting was performed using the primary antibodies listed in *Table* S1. For further details, refer to the *Supporting information*.

RNA interference and TOP/FOP-flash reporter assay

C2C12 cells were transfected with 20-pmol small interfering RNAs (siRNAs) for 24 h using Lipofectamine 2000 (Invitrogen, Carlsbad, CA, USA). For the reporter assay, C2C12 cells were co-transfected with a TOP/FOP-flash reporter plasmid (provided by Dr Aimee D. Kohn, SCCA Evergreen Health, Kirkland, WA, USA) and a control reporter plasmid pRL-TK (Promega, Madison, WI, USA) for 24 h using Lipofectamine 2000, followed by treatment with or without 1-μg/mL SLIT3 for 24 h. For further details, refer to the *Supporting information*.

Semiquantitative RT–PCR and real-time PCR

Total RNA was isolated using TRIzol™ reagent (Invitrogen), and cDNA was synthesized using Superscript® III First-Strand Synthesis System (Invitrogen), according to the manufacturer's instructions. Primer sequences for semiquantitative RT–PCR are listed in *Table* S2. Real-time PCR was performed on LightCycler 480® (Roche, Mannheim, Germany), using LightCycler® 480 SYBR Green I Master Mix (Roche). Primers used for real-time PCR are listed in *Table* S3. The TaqMan probes (Invitrogen) of Mm00483191_m1, Mm01162497_m1, Mm00483039_m1, and Hs03928990_g1 were used to investigate the expression of *M-cadherin*, *N-cadherin*, *Ctnnb1*, and *18S rRNA*, respectively.

Receptor-binding assay

Receptor-binding assay was performed as described previously.[5] Briefly, the indicated amounts of the C2C12 cell lysates were exposed to SLIT3 or BSA by incubating them in 10 μg/mL SLIT3- or BSA-coated wells for 2 h. The plate was washed and blocked with 1% BSA in PBST and was incubated with antibodies against Robo1 or Robo2 for 2 h. The colorimetric signal was generated using the HRP-TMB (3,3′,5,5′-tetramethylbenzidine) system.

Statistical analysis

In vitro data are expressed as mean ± standard error of at least three independent experiments in triplicate to show an uncertainty of mean estimator. Animal works are expressed as mean ± standard deviation to show its dispersion, and provided individual values within the bar graphs. Differences between two groups were examined using an unpaired *t* test, and differences among three or more groups

were examined using the Kruskal–Wallis test followed by Bonferroni correction. All statistical analyses were performed using SPSS software, version 21.0 (Chicago, IL, USA), and $P < 0.05$ was considered significant.

Results

Skeletal muscle alterations in Slit3-deficient mice

The body weight of male $Slit3^{-/-}$ mice was lower than that of the wild-type (WT) littermates (*Figure* 1A). Dual-energy X-ray absorptiometry showed that lean mass was significantly lower in the $Slit3^{-/-}$ mice than that in the WT littermates; however, no difference was observed in the fat mass (*Figure* 1B). $Slit3^{-/-}$ mice had significantly lower all muscle weights than the WT littermates (*Figure* 1C). Further, the relative masses of the GC and SOL muscles were significantly lower in the $Slit3^{-/-}$ mice ($0.580 \pm 0.039\%$ and $0.033 \pm 0.003\%$, respectively) than those in the WT littermates ($0.622 \pm 0.043\%$ and $0.038 \pm 0.003\%$, respectively) (all, $P < 0.05$) (*Figure* 1D). Skeletal muscle strength and physical activity were evaluated using grip strength (*Figure* 1E) and wheel-running tests (*Figure* 1F), respectively. $Slit3^{-/-}$ mice exhibited a significant decrease in the grip strengths in the forelimb and four paws, and they also ran a shorter distance compared with their WT littermates. Female $Slit3^{-/-}$ mice, similar to male $Slit3^{-/-}$ mice, had lower muscle weight and grip strengths, and ran shorter distances than their WT littermates (*Figure* S1). These results suggest that SLIT3 may be an essential factor for maintaining the skeletal muscle mass, strength, and physical activity.

Next, the tissue architecture of the GC muscle of the $Slit3^{-/-}$ mice and their WT littermates was investigated using H&E staining (*Figure* 2A). The cross-sectional area (CSA) of the GC muscle fibres was significantly lower in the $Slit3^{-/-}$ mice than that in the WT littermates. Similar results were obtained for the EDL muscle (*Figure* 2B). The CSA of muscle fibres in the male $Slit3^{-/-}$ mice was approximately 35.3–41.3% lower than that in the WT littermates. Myonuclei number per CSA was also lower in the $Slit3^{-/-}$ mice (*Figure* 2C). Furthermore, the number of Type I and Type IIa fibres, but not of Type IIb and Type IIx fibres, in the GC muscle of $Slit3^{-/-}$ mice was significantly decreased compared with that of their WT littermates (*Figure* 2D). IF staining was performed to detect sarcolemma of muscle fibre and satellite cells using antibodies against laminin and PAX7, respectively (*Figure* 2E). No difference was observed in the number of satellite cells per fibre in the GC muscle between the $Slit3^{-/-}$ mice and their WT littermates. *Pax7* mRNA expression levels were also similar in the GC muscle between the two genotypes (*Figure* 2F). These results indicate that SLIT3 is mainly involved in skeletal muscle mass but not in satellite cell recruitment, especially in Type I and Type IIa muscle fibres.

We previously reported that *Slit3* is expressed in several organs, with the highest expression levels in bone and brain.[5] *Slit3* expression levels in the skeletal muscle were significantly lower compared to bone (*Figure* S2A). Furthermore, SLIT3 was secreted at low levels even in *Slit3*-overexpressed myoblasts (*Figure* S2B); and its overexpression did not alter *in vitro* myogenesis (*Figure* S2C). Therefore, we examined the effect of extracellular SLIT3 on muscle cell function.

SLIT3 enhances myoblast differentiation by activating β-catenin signalling

Differentiation of C2C12 myoblasts into myotubes was enhanced upon treatment with recombinant SLIT3 (*Figure* 3A). SLIT3 also increased their fusion and increased the number of larger myotubes but decreased that of smaller myotubes (*Figure* 3B). In contrast, SLIT3 treatment did not affect the viability (*Figure* S3A) and proliferation (*Figure* S3B) of myoblasts. These results suggest that SLIT3 enhances myogenesis by stimulating myoblast differentiation rather than by altering its population.

Several factors, such as myogenic regulatory factor (MRF) 4, myogenic factor 5, myoblast determination protein 1 (MyoD), myogenin, and myocyte enhancer factors 2A and 2C, regulate myoblast differentiation.[12] SLIT3 stimulated the expression of *myogenin* mRNA but not that of the other genes in the C2C12 myoblasts (*Figure* S3C). Immunocytochemistry confirmed that SLIT3 increased the number of myogenin$^+$ cells (*Figure* 3C).

SLIT ligands are known to modulate β-catenin[13] and AKT[14] activities. Activated β-catenin and AKT can induce myoblast differentiation and myogenesis.[15,16] SLIT3 did not activate AKT in myoblasts (*Figure* S4A), but it induced β-catenin signalling in the myoblasts (*Figure* 4A and 4B). SLITs could also inhibit β-catenin signalling, particularly in cancer cells.[14,17] SLIT3 stimulated β-catenin signalling in myoblasts and osteoblasts, but suppressed it in breast and liver cancer cells (*Figure* S4B), suggesting that SLIT3-induced activation of β-catenin signalling is cell type-dependent. The knockdown of β-catenin almost completely blocked the SLIT3-induced myotube formation (*Figure* 4C), and reversed the SLIT3-induced changes in myogenin expression at the mRNA (*Figure* 4D) and protein levels (*Figure* 4E) in the myoblasts. Next, we evaluated the SLIT3's effect on other factors connected to β-catenin. SLIT3 up-regulated nephrin levels (*Figure* S5A) but did not have any effect on *c-Myc* (*Figure* S5B) or AMP-activated protein kinase, as well as the lipidation of autophagy marker LC3B (*Figures* S5C and S5D). We focused here on the mechanisms involved in SLIT3-induced up-regulation of myogenin.
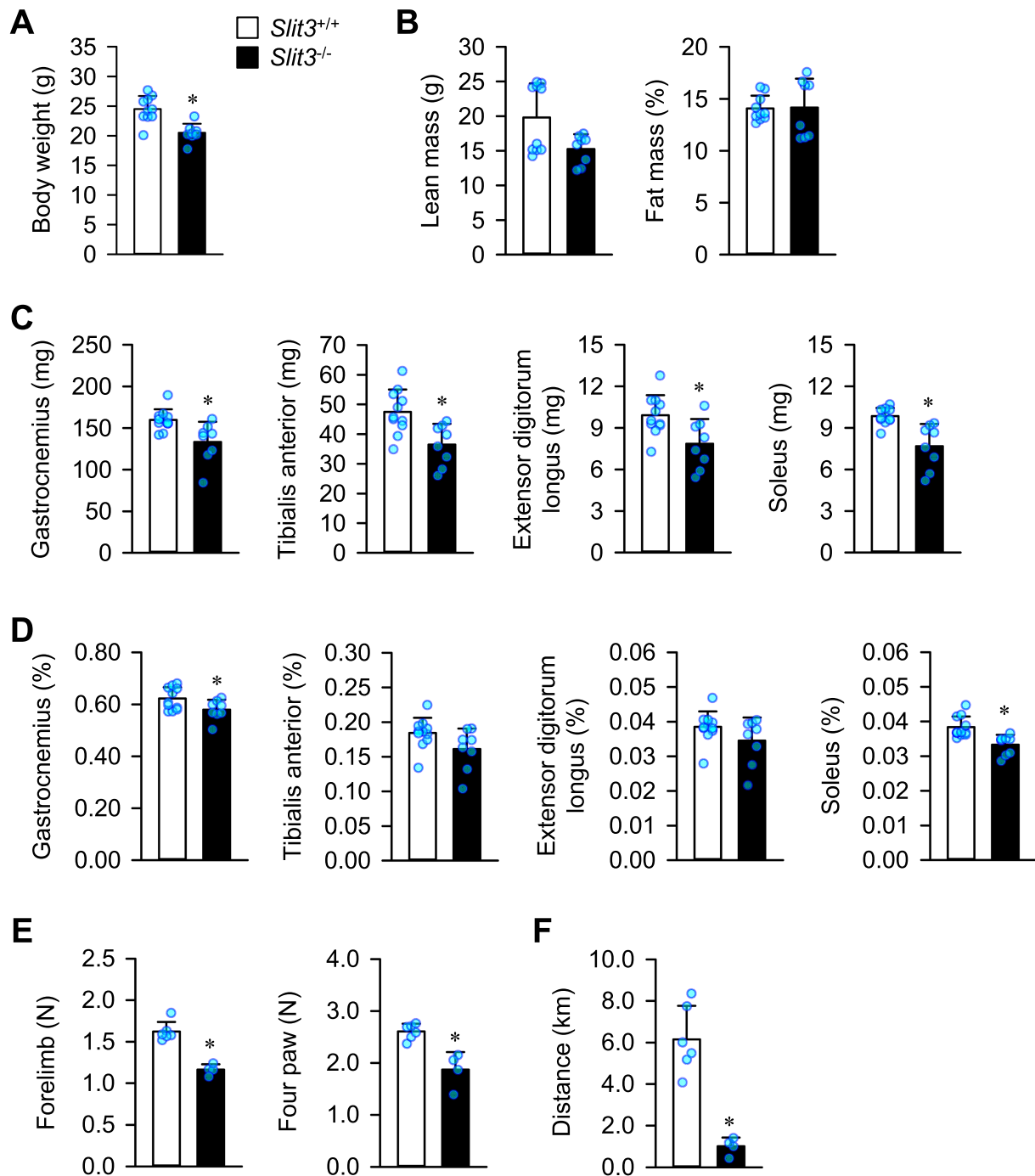
Figure 1 Reduced skeletal muscle mass, strength, and physical activity in the *Slit3*$^{-/-}$ mice. *(A)* Body weight and *(B)* lean and fat mass of the 7-week-old male *Slit3*$^{-/-}$ mice and their WT littermates (*n* = 8–10 per group) were determined using dual-energy X-ray absorptiometry. Percentages of fat mass were calculated by dividing their raw values by the body weight. *(C,D)* The muscle mass of the mice was expressed as raw values *(C)* and as the percentage of body weight (also referred to as relative muscle mass) *(D)* (*n* = 8–11 per group). *(E,F)* Skeletal muscle strengths and physical activity were determined based on the grip strength of the forelimbs and four paws *(E)* and daily wheel-running distance *(F)*, respectively (*n* = 4–6 per group). *P* < 0.05 compared with the wild-type littermates using the unpaired *t* test.

We further characterized the mechanism of SLIT3-mediated β-catenin stimulation. Wnt3a, similar to SLIT3, increased myogenesis (*Figure* S6A). However, Wnt3a, but not SLIT3, elevated the levels of phosphorylated GSK-3β and LRP6; and SLIT3, but not Wnt3a, increased the levels of β-catenin phosphorylated at Y489 (*Figure* S6B). These results suggest that SLIT3 and Wnt3a activate β-catenin signalling *via* different mechanisms. The binding of SLIT ligands to their
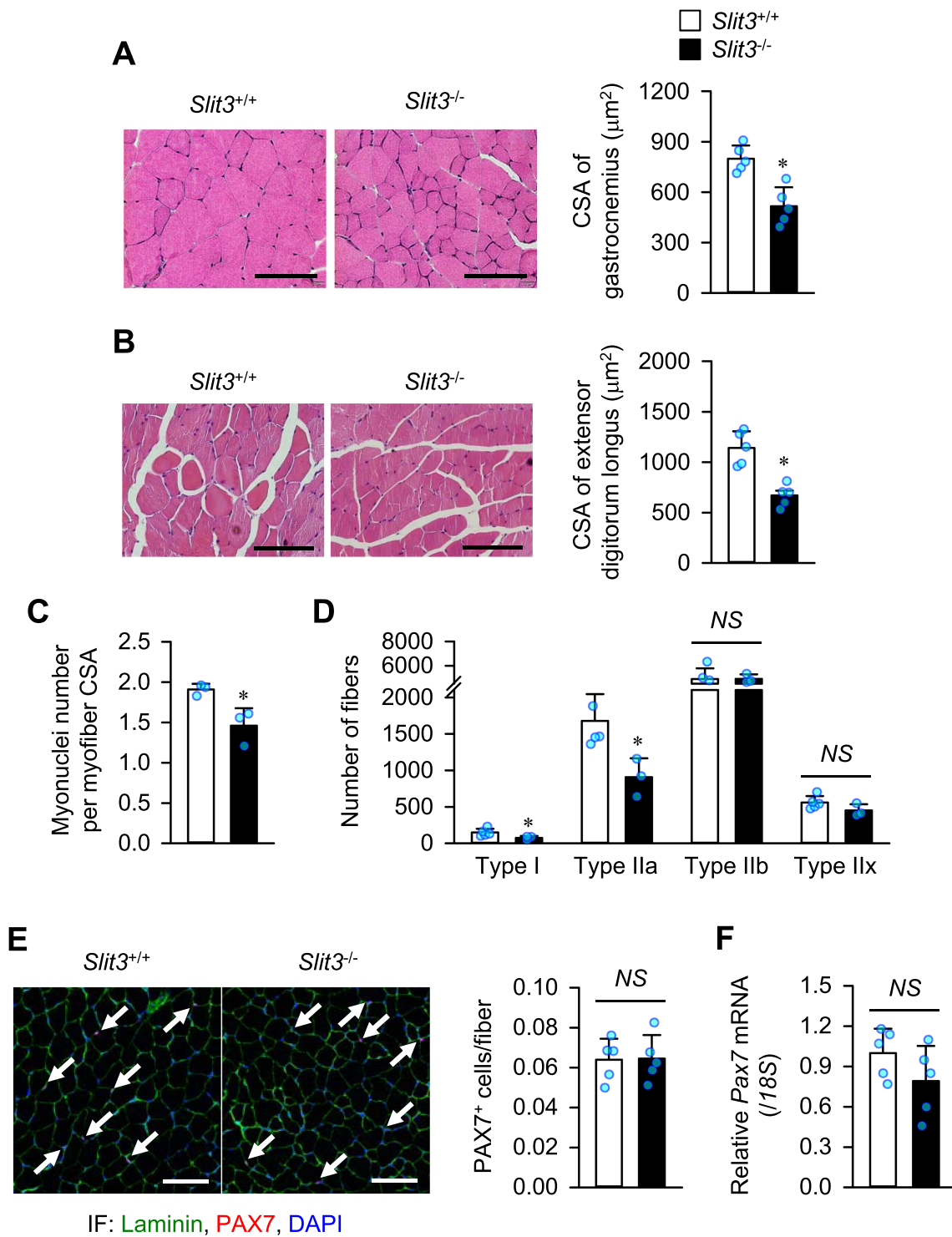
Figure 2 Histology of the skeletal muscle of the $Slit3^{-/-}$ mice. (A–C) Haematoxylin and eosin staining of the (A) gastrocnemius and (B) extensor digitorum longus muscles of the 7-week–old male $Slit3^{-/-}$ and their wild-type littermates (n = 5 per group). Myonuclei number per myofibre CSA (n = 3 per group) in the gastrocnemius muscle was shown (C). (D) Quantification of immunopositive MyHC isoforms in the gastrocnemius muscle. (E) Immunofluorescence was performed to check laminin (green) and PAX7 (red) expression in the gastrocnemius muscles; DAPI (blue) was used to counterstain the nuclei. Arrows indicate PAX7$^+$ cells. Respective quantitative results are shown in the right panels. (F) Pax7 mRNA expression in the gastrocnemius muscle was determined by real-time PCR. Scale bars: 100 μm. *$P < 0.05$ compared with the wild-type littermates using the unpaired t-test. CSA, cross-sectional area; NS, not significant.
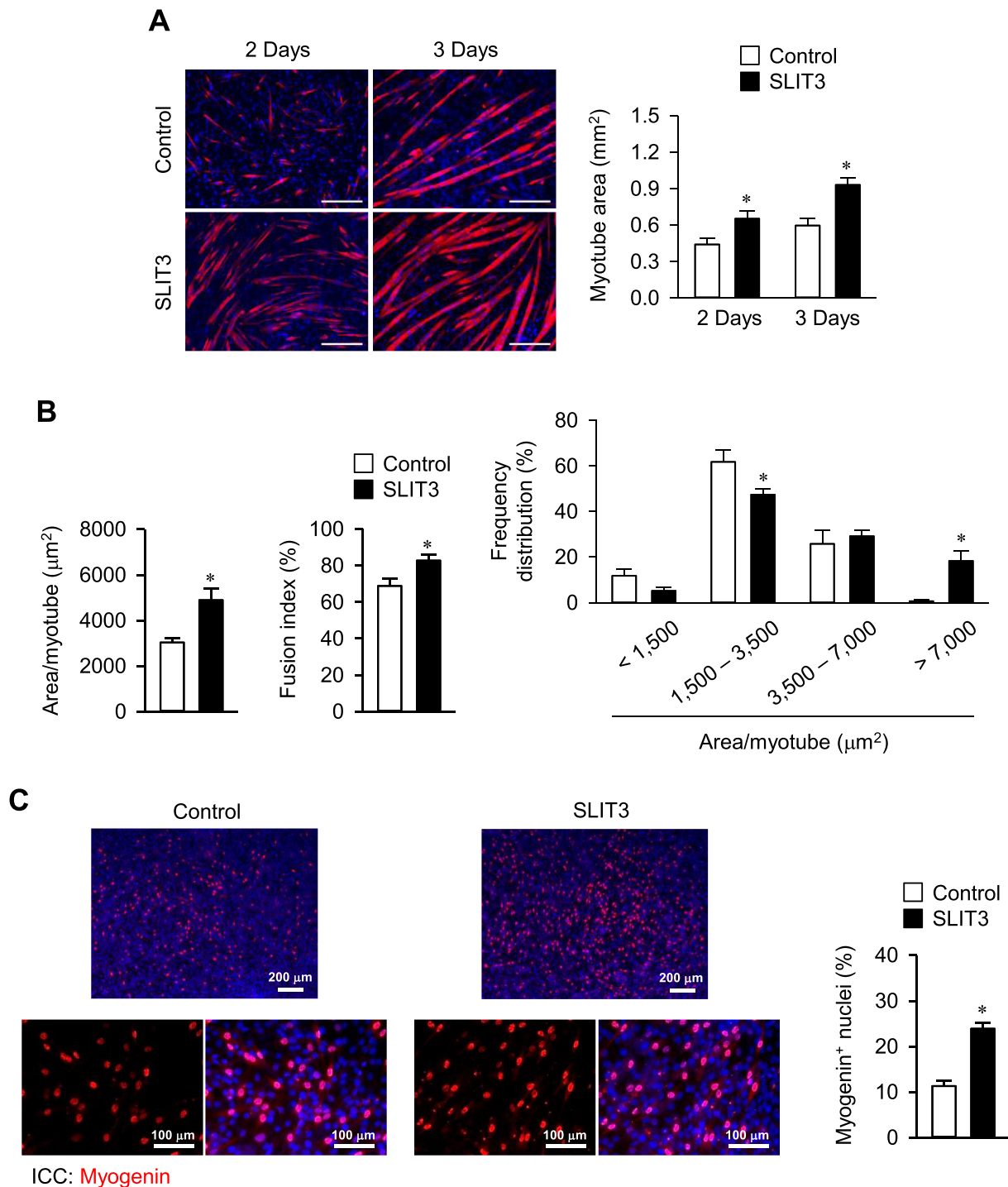
Figure 3 SLIT3 stimulates myoblast differentiation and myogenin expression *in vitro*. *(A,B)* C2C12 myoblasts were differentiated in the presence or absence of 1 μg/mL SLIT3 for 2 or 3 days. *(A)* Myotubes were immunostained with the anti-myosin heavy chain (MyHC) antibody, and the nuclei were counterstained with DAPI. The total myotube area is shown in the right panel. Scale bars: 200 μm. *(B)* MyHC area per myotube, fusion index, and frequency distribution of myotube were determined from the fast type of myotubes. Fusion index (%) was calculated as described in the *Supporting information*. *(C)* Immunocytochemistry analysis of myogenin expression in the C2C12 myoblasts treated with 1 μg/mL SLIT3 for 24 h. Quantitative results are shown in the right panel. *P < 0.05 compared with the untreated control cells using the unpaired *t* test or Kruskal–Wallis test followed by Bonferroni correction.
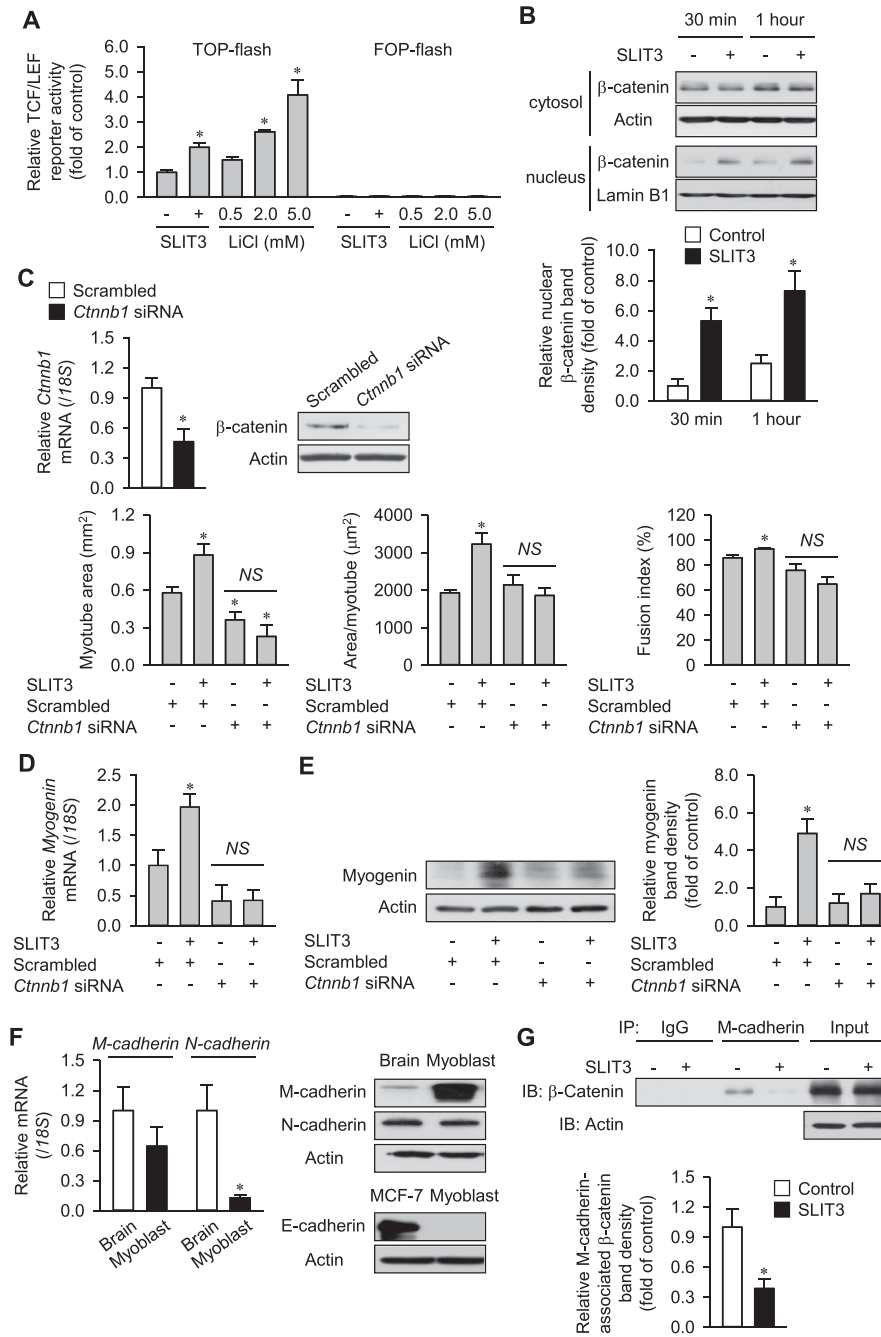
Figure 4 Activation of β-catenin signalling mediates SLIT3-stimulated myoblast differentiation. (A) C2C12 myoblasts were treated with 1 μg/mL SLIT3 for 18 h, and β-catenin promoter activity was measured by performing the TOP/FOP flash reporter assay. LiCl was used as a positive control. *(B)* C2C12 myoblasts were treated with 1 μg/mL SLIT3 for the indicated times, and cytosolic and nuclear extracts were prepared for western blotting with an anti-β-catenin antibody. Quantitative results are shown in the lower panel. *(C–E)* C2C12 myoblasts were transfected with the β-catenin siRNA, as described in the *Supporting information*. *(C)* the results of the real-time PCR and western blotting of β-catenin expression after the siRNA transfection are shown in the upper panel. The lower panel shows the results of total myotube area, area/myotube, and fusion index after the treatment of the siRNA-transfected C2C12 cells with or without 1 μg/mL SLIT3 for 2 days. Myotubes were stained with anti-fast MyHC antibody. *(D,E)* The results of the real-time PCR *(D)* and western blotting *(E)* of myogenin after the treatment of the siRNA-transfected C2C12 cells with or without 1 μg/mL SLIT3 for 24 h are shown. The right panel shows the results of western blotting. *(F)* The M-, N-, and E-cadherin mRNA and/or protein expressions in the myoblasts were determined by real-time PCR and western blotting, respectively. Brain tissue and MCF-7 (a breast cancer cell line) were used as positive controls. *(G)* C2C12 cells were treated with or without 1 μg/mL SLIT3 for 30 min. Total cell lysates (500 μg protein) were immunoprecipitated with the anti-M-cadherin antibody, and the immunoprecipitated complexes were analysed by performing western blotting with the anti-β-catenin antibody. Actin was used as a loading control. Quantitative results are shown in the lower panel. $*P < 0.05$ compared with the untreated control cells or brain tissue using the unpaired t test or Kruskal–Wallis test followed by Bonferroni correction. *NS*, not significant.

receptor results in the dissociation of a multimolecular complex containing the SLIT receptor and cadherin; this results in the dissociation of β-catenin from cadherin and subsequent activation of β-catenin. We observed that myoblasts predominantly expressed M-cadherin at both mRNA and protein (*Figure* 4F). We confirmed that SLIT3 decreased the M-cadherin-associated β-catenin level in myoblasts (*Figure* 4G). Upon SLIT binding to ROBO, Cables is recruited to the ROBO-associated Abl kinase, resulting in the phosphorylation of β-catenin at Y489 which has decreased affinity for cadherins.[13] We observed that SLIT3 treatment increased the levels of M-cadherin-associated Cables and phosphorylated β-catenin at Y489 in a time-dependent and consecutive manner (*Figure* S7). These results indicate that SLIT3 increased the level of active β-catenin by promoting its dissociation from M-cadherin in myoblasts, which in turn increases myogenin expression to induce myoblast differentiation.

ROBO2 is a putative receptor for SLIT3 in myoblasts

The SLIT receptor Roundabout (ROBO) family contains four members, namely, ROBO1-4.[18] We detected the expression of *Robo1* and *Robo2*, but not *Robo3* and *Robo4*, in the myoblasts (*Figure* 5A). Further analysis showed that *Robo2* was ubiquitously expressed in several tissues and organs (*Figure* S8). ELISA revealed that ROBO1 and ROBO2 may bind to SLIT3 in myoblasts (*Figure* 5B). *Robo2* knockdown almost completely reversed the SLIT3-induced myotube formation, but *Robo1* knockdown did not (*Figure* 5C). Further, *Robo2* knockdown blocked the SLIT3-induced myogenin expression in myoblasts, but *Robo1* knockdown did not (*Figure* 6A). We also noted that SLIT3-stimulated β-catenin was mediated by ROBO2 (*Figure* 6B). Collectively, these results indicate that ROBO2—but not ROBO1—mediates the SLIT3-induced myoblast differentiation *via* the up-regulation of β-catenin signalling and myogenin. However, we could not confirm this *in vivo* because *Robo2*$^{-/-}$ mice are embryonically lethal.[3]

Recombinant SLIT3 fragment can act as a novel therapeutic agent against muscle loss

Human SLIT3 has a molecular weight of approximately 170 kDa and contains 1523 amino acids. This large size may be disadvantageous for drug development. SLIT3 contains four LRRDs, and the second LRRD (LRRD2)—containing 130 amino acids—binds to the ROBO receptors.[19–21] Therefore, we examined whether SLIT3 LRRD2 could be used as an agent for treating muscle loss. We observed that similar to the full-length SLIT3, SLIT3 LRRD2 induced myotube formation (*Figure* 7A) and myogenin expression (*Figure* 7B) and reduced the levels of M-cadherin-bound β-catenin (*Figure* 7C). SLIT3

LRRD2 treatment did not affect protein synthesis and degradation levels, and the expressions of their related signalling events in myoblasts (*Figures* S9A and 9B). The signalling expressions were also comparable between muscles of *Slit3*$^{-/-}$ mice and their WT littermates (*Figure* S9C).

To test the *in vivo* effects of SLIT3 LRRD2, we used two well-established mouse models characterized by muscle loss: estrogen-deficient ovariectomized (OVX) and aged mice. First, OVX mice were intravenously injected with SLIT3 LRRD2 for 4 weeks. Blood SLIT3 concentrations (*Table* S4) and muscular *Slit3* levels (*Figure* S9D) were similar between the treated and untreated OVX mice. SLIT3 LRRD2 administration in OVX mice resulted in increased muscle masses of GC and SOL (by 9.4%) and TA and EDL (by 18.4%) compared to those in untreated OVX mice (*Figure* 8A), showing increased relative muscles masses by 10.0% and 20.1%, respectively. However, body weights were similar between the treated and untreated OVX mice. The H&E staining of the GC muscle showed that SLIT3 LRRD2 treatment increased the size of muscle fibres in OVX mice (*Figure* 8B).

Because *Robo2* is ubiquitously expressed (*Figure* S8), SLIT3 LRRD2 may also have an effect on other organs. All organs, such as heart, kidney, brain, lung, thymus, liver, spleen, stomach, and intestine, were grossly normal after the treatment of SLIT3 LRRD2 in the OVX mice. All blood biochemical parameters, including renal and liver functions, were similar between the two OVX groups (*Table* S5). ROBO2 is known to be involved in heart and kidney development.[3,22] H&E staining did not show any apparent differences in both two organs, between the untreated and treated mice (*Figure* S10A). The SLIT3 LRRD2 treatment increased the expression level of active β-catenin in the GC muscle and in the heart (*Figure* S10B) but not in the kidney (data not shown). However, the number of β-catenin$^+$ cells, both before and after the treatment, appeared to be higher in the GC muscle than in the heart.

Next, we evaluated the aged mouse model. *Figure* 8C shows the muscle masses in aged mice. Untreated aged mice exhibited a higher body weight but lower relative masses of all the investigated muscles than the young mice. SLIT3 LRRD2 treatment significantly increased the relative masses of the GC and SOL muscles by 7.8% and 18.0%, respectively, in the aged mice (*Figure* 8C). The relative masses of the GC and SOL muscles were significantly higher in the treated aged mice (0.548 ± 0.045% and 0.033 ± 0.005%, respectively) than in the untreated aged mice (0.508 ± 0.016% and 0.028 ± 0.003%, respectively) (all, $P < 0.05$). The untreated aged mice exhibited a remarkable decrease in hanging duration (by ~90%) compared with the young mice. These results indicate that aging induces a greater decline in skeletal muscle function than that predicted based on changes in the muscle mass. SLIT3 LRRD2 treatment markedly increased the hanging duration of the aged mice by approximately 1.7-fold. We assessed the morphology of muscle fibres. SLIT3
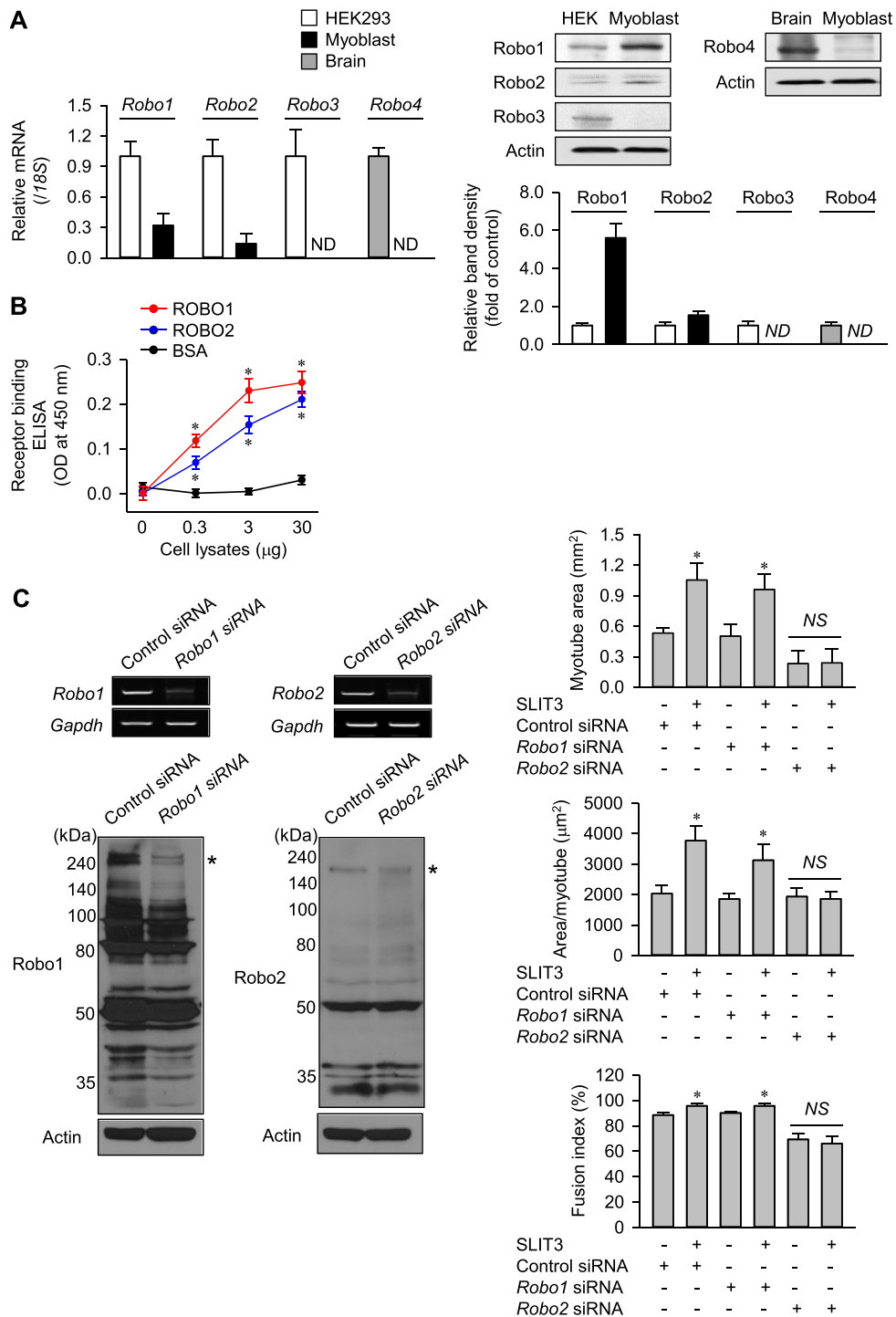
Figure 5 ROBO2 mediates SLIT3-stimulated myoblast differentiation. *(A)* The mRNA and protein expressions of the Robo isotypes in C2C12 myoblasts were determined by performing real-time PCR and western blotting, respectively. HEK293 cells and brain tissue were used as positive controls for Robo1–3 and Robo4, respectively. Quantitative results are shown in the lower right panel. *(B)* Interaction of SLIT3 with ROBO1 and ROBO2 in the C2C12 myoblast using a binding ELISA assay. Various amounts of the C2C12 cell lysates were incubated for 2 h into 10 μg/mL SLIT3- or bovine serum albumin-coated wells, followed by quantification of ROBO1 and ROBO2 by ELISA. *(C)* The results of semiquantitative RT-PCR and western blotting of Robo1 or Robo2 expression after the siRNA transfection are shown in the left panel. Uncropped western blots are shown to confirm the down-regulation of specific Robo1 and Robo2 bands (indicated by asterisks). The right panel shows the results of total myotube area, area/myotube, and fusion index after the treatment of the siRNA-transfected C2C12 cells with or without 1 μg/mL SLIT3 for 2 days. Myotubes were stained with anti-fast MyHC antibody. *$P < 0.05$ compared with the SLIT3-untreated control cells using the unpaired *t* test or Kruskal–Wallis test followed by Bonferroni correction. *ND*, not detected; *NS*, not significant.
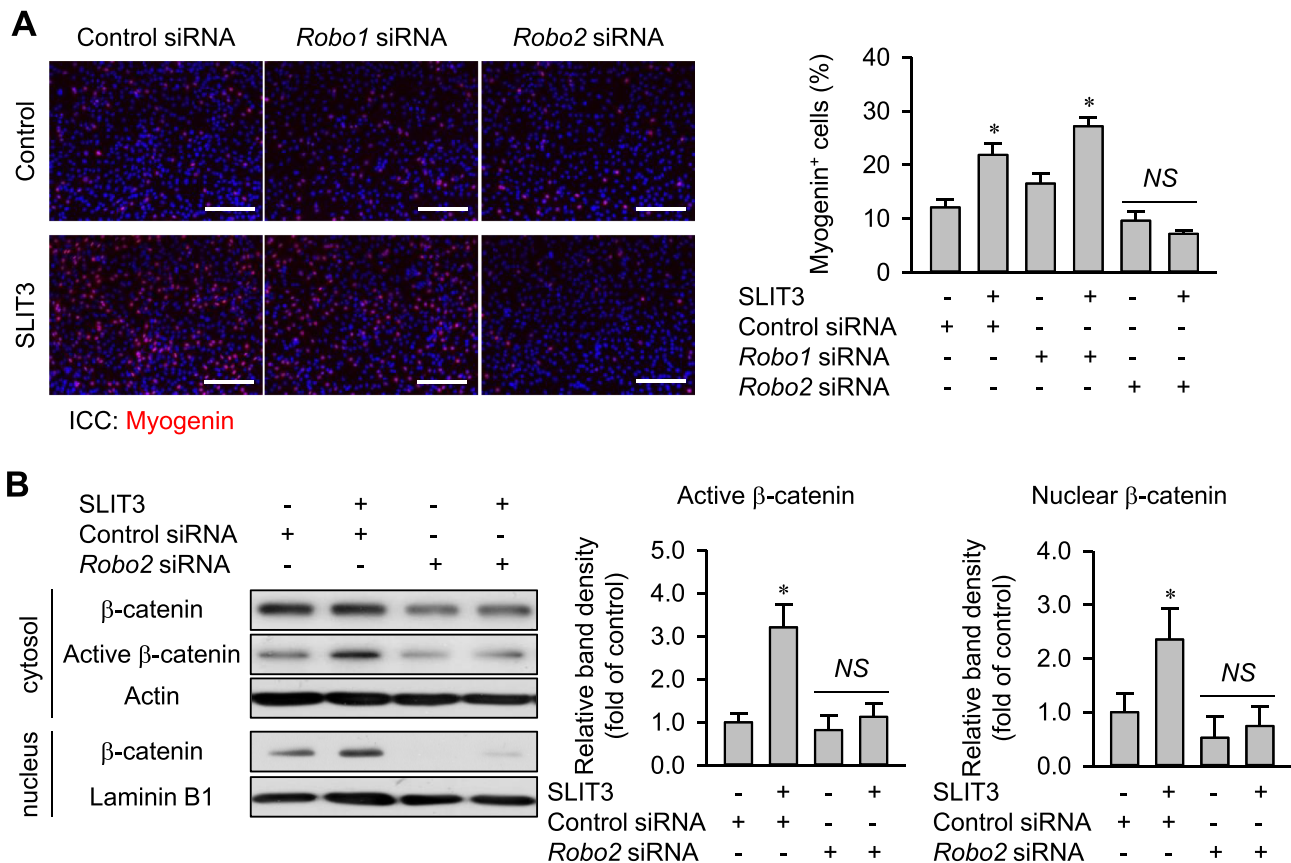
Figure 6 ROBO2 mediates the SLIT3-stimulated myogenin expression and activation of β-catenin signalling. C2C12 myoblasts were transfected with the siRNAs targeting *Robo1* and *Robo2*, as described in the *Supporting information*. (A) Immunocytochemistry analysis of myogenin expression in the siRNA-transfected C2C12 cells treated with 1 μg/mL SLIT3 for 24 h. Quantitative results are shown in the right panel. Scale bars: 500 μm. (B) The siRNA-transfected C2C12 cells were treated with 1 μg/mL SLIT3 for 1 h. Cytosolic and nuclear extracts were prepared for western blotting with their relevant antibodies. Quantitative results are shown in the right panels. *$P < 0.05$ compared with the untreated control cells using the Kruskal–Wallis test followed by Bonferroni correction. *NS*, not significant.

LRRD2 treatment increased the size of muscle fibres and myonuclei number per CSA in aged mice (*Figure* 8E). We also labelled the sarcolemma in the SOL muscle using wheat germ agglutinin (WGA) (*Figure* 8F). Because WGA binds to glycoproteins found on cell plasma membranes, WGA is routinely used for sarcolemma staining to determine CSA. We found that SLIT3 LRRD2 treatment increased the CSA of SOL muscle fibres in the aged mice.

In vivo pharmacokinetics of SLIT3 LRRD2

Five transitions of light peptide and SIS peptide for SLTSLVLYGNK were determined after CE optimization using Skyline software based on triple quadrupole LC–MS (*Figure* S11A). Final multiple reaction monitoring (MRM) method is shown in *Table S*6. In final quantitation analysis, transitions for light peptide (Q1: 597.8401^{++}, Q3: 994.5568^{+++}) and SIS peptide (Q1: 601.8472^{++}, Q3: 994.5568^{+++}) were selected for quantitation (*Figure* S11B). Covariance of peak area and

retention time variability for triplicate MRM run were 4.5% and 1.7%, respectively, indicating reproducibility of MRM analysis. R^2 was 0.9834, and the lower limit of quantitation was 8.9 ng/mL based on a response curve. SLIT3 LRRD2 levels at 0, 2, 4, 6, 8, and 24 h were below the lower limit of quantitation (*Figure* S11C). The non-compartmental analysis of the concentration-time profiles was applied to calculate pharmacokinetic parameters (*Table* S7). The half-life was 0.54 ± 0.10 h.

Discussion

We have shown here that *Slit3* deficiency decreased the skeletal muscle mass *in vivo*. SLIT3 stimulated myoblast differentiation by activating β-catenin signalling and up-regulating myogenin *in vitro* (*Figure* S12). SLIT3 LRRD2 treatment increased the skeletal muscle mass and/or function in the sex-hormone–deficient and aged mice. Thus, our findings
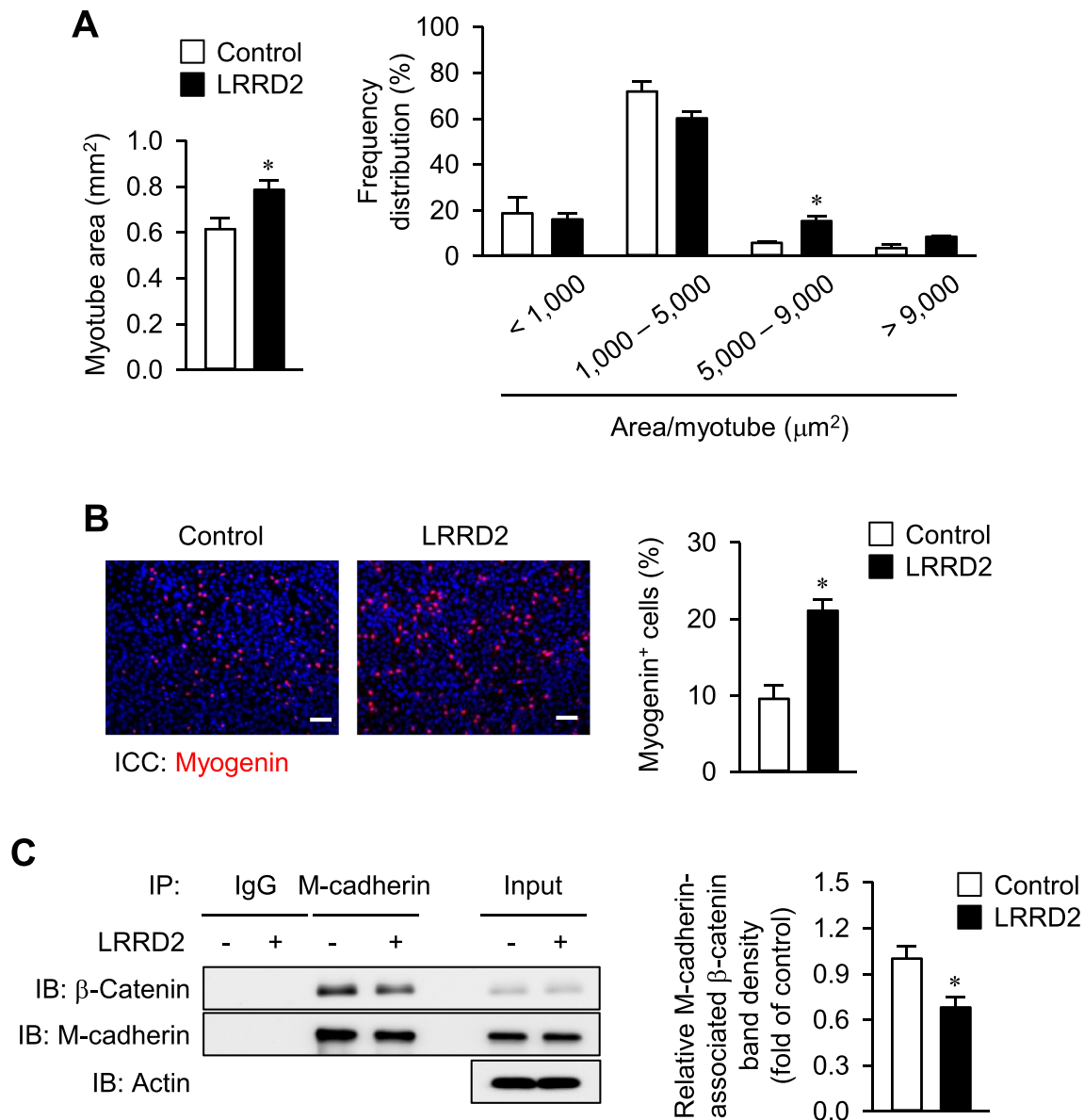
Figure 7 SLIT3 LRRD2 stimulates myoblast differentiation. *(A)* C2C12 myoblasts were treated with 10-nM SLIT3 LRRD2 for 3 days. Myotubes were stained with anti-fast MyHC antibody. The frequency distribution of the myotube area is shown in the right panel. *(B)* Immunocytochemistry ICC analysis of myogenin expression in C2C12 myoblasts treated with 10-nM SLIT3 LRRD2 for 24 h. Scale bars: 200 μm. Quantitative results are shown in the right panel. *(C)* C2C12 myoblasts were incubated in the presence or absence of 10-nM SLIT3 LRRD2 for 30 min. Total cell lysates (500-μg protein) were immunoprecipitated with the anti-M-cadherin antibody, and the immunoprecipitated complexes were analysed by performing western blotting. Quantitative results are shown in the right panel. *P < 0.05 compared with the untreated control cells using the unpaired *t* test or Kruskal–Wallis test followed by Bonferroni correction.

provide novel insights into the involvement of SLIT3 in skeletal muscle biology and suggest that SLIT3 LRRD2 can be developed as a therapeutic agent against muscle loss. A previous study[23]—and ours[5]—have shown that SLIT3 performs an osteoprotective role *through* various mechanisms and that SLIT3 LRRD2 exerts therapeutic effects against osteoporosis.[5] These findings indicate that SLIT3 LRRD2 can be developed as a drug that targets both osteoporosis and sarcopenia.

The SLIT/ROBO system is a component of multiple signalling pathways, including the Wnt/β-catenin and PI3K/AKT cascades.[24] Although PI3K/AKT signalling are critical in myogenesis,[25] SLIT3 did not activate the PI3K/AKT pathway in myoblasts. Activation of β-catenin induces myoblast differentiation,[15] and we found that SLIT3 activated this pathway in myoblasts. Rhee *et al.*[13] reported that SLIT ligands release N-cadherin-associated β-catenin, resulting in its activation. Upon binding to SLIT, ROBO-associated Abl recruits
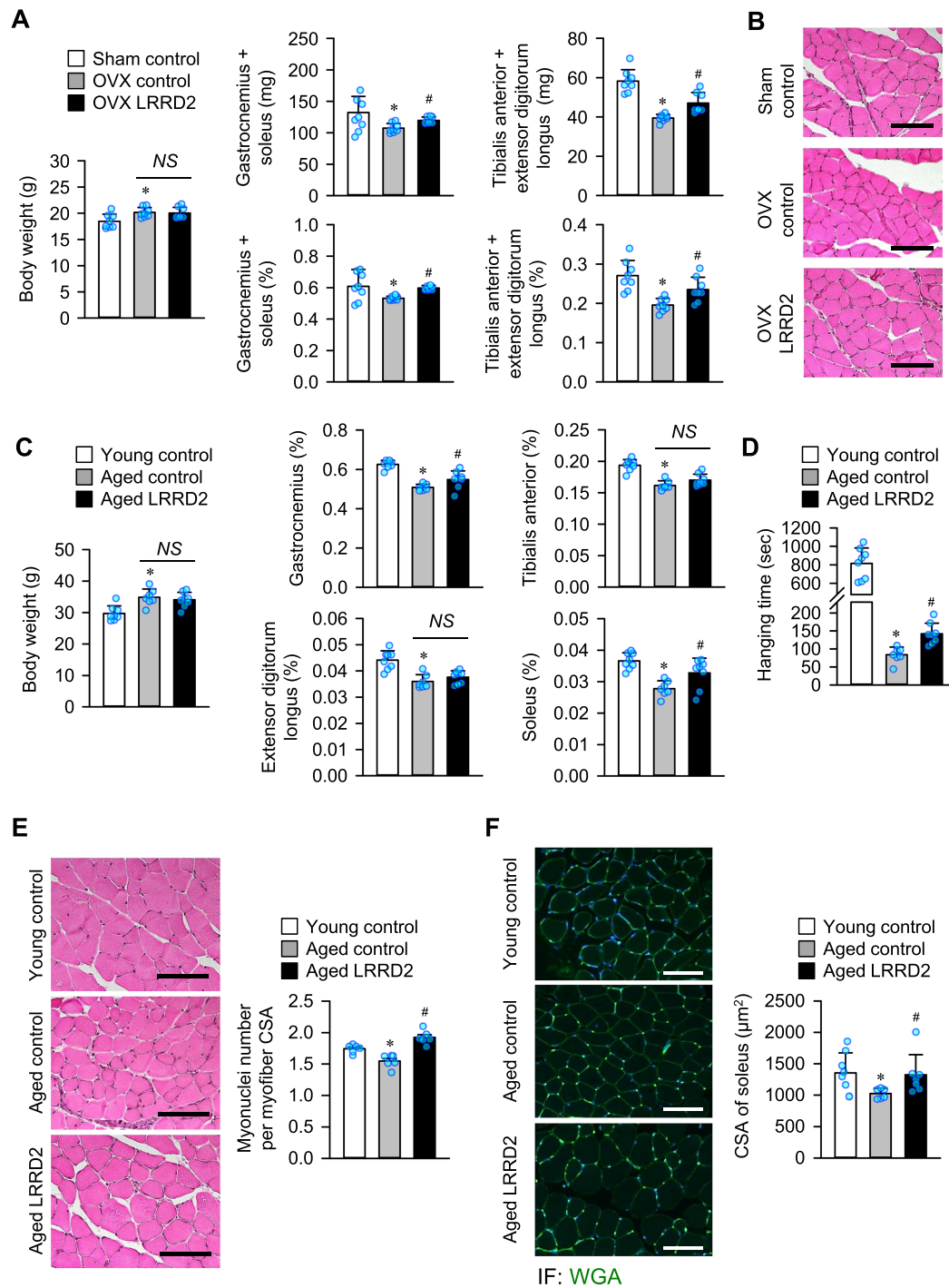
Figure 8 SLT3 LRRD2 prevents muscle loss *in vivo*. *(A,B)* Ovariectomized (OVX) mice (*n* = 8 per group) were intravenously injected with phosphate-buffered saline or 10-μg SLIT3 LRRD2 for 4 weeks, as described in the *Supporting information*. The mice were sacrificed, and their muscles were removed and weighed immediately. Muscle mass was expressed as raw values and as the percentage of body weight (also referred to as relative muscle mass) *(A)*, and haematoxylin and eosin staining of the gastrocnemius muscle are shown *(B)*. *(C–F)* Six- or 18-month-old male C57BL/6 mice (*n* = 7–8 per group) were intravenously injected with phosphate-buffered saline or 10-μg SLIT3 LRRD2 for 4 weeks. The mice were sacrificed, their muscles were removed and weighed immediately, and relative muscle masses of the muscles were expressed *(C)*. A four-limb hanging test was performed, and the hanging duration is shown *(D)*. Haematoxylin and eosin staining of the gastrocnemius muscle and myonuclei number per myofibre cross-sectional area *(E)*. Sections of the soleus muscle were stained with the FITC-labelled wheat germ agglutinin *(F)*. A representative image showing the immunofluorescence staining. The quantitative results of the cross-sectional areas of the soleus muscle are shown in the right panel. **P* < 0.05 compared with the sham-operated or young control mice and *#P* < 0.05 compared with the untreated OVX or aged control mice using the Kruskal–Wallis test followed by Bonferroni correction. *NS*, not significant. Scale bars: 100 μm.

Cables, which in turn facilitates the phosphorylation of β-catenin by Abl at tyrosine 489. β-Catenin phosphorylated at Y489 exhibits decreased affinity for N-cadherin. We observed that M-cadherin was more prominently expressed than N-cadherin in myoblasts and that SLIT3 activated β-catenin signalling by promoting its dissociation from M-cadherin.

In the present study, SLIT3 treatment resulted in increased myogenin expression *via* activation of β-catenin signalling. We also noted the decreased and increased myonuclei number in $Slit3^{-/-}$ and LRRD2-treated mice, respectively, suggesting a crucial role of SLIT3 on fusion of myogenic cells. The Wnt/β-catenin signalling pathway plays an essential role in muscle development in embryos—and skeletal muscle homeostasis—in adults.[26] β-Catenin activations stimulated differentiation of satellite cells and myoblasts,[27,28] and muscle fibre hypertrophy.[28,29] Although their mechanisms should be further elucidated, one of the signalling pathways, the induction of MRFs including myogenin,[30,31] is of particular interest to our study. Pan *et al.*[32] reported that β-catenin directly binds to—and activates—the cis-elements in the MyoD promoter. Myogenin—a member of the MyoD family of transcription factors that is essential for myoblast differentiation[33]—is a MyoD target; therefore, β-catenin activation increases myogenin expression. Jones *et al.*[31] reported that β-catenin activation promoted myoblast fusion and differentiation by increasing myogenin expression. These findings are consistent with the results obtained in the present study.

In addition, it has been reported that β-catenin regulates skeletal muscle development and myoblast fusion by increasing nephrin expression level.[34,35] Although we did not examine the precise role of nephrin in SLIT3-induced myogenic differentiation, it is possible that increased nephrin expression level could be the other mechanism involved in myogenesis, because we observed that SLIT3 treatment stimulated myoblast fusion and nephrin expression. Furthermore, we observed that Type I (slow-twitch, oxidative) and Type IIa (fast-twitch, oxidative) muscle fibres, but not Type IIb (fast-twitch, glycolytic) and Type IIx (fast-twitch, oxido-glycolytic) fibres, were reduced in muscles of *Slit3*-deficient mice, suggesting that SLIT3 plays a role in oxidative phosphorylation in muscle cells. Lastly, given the role of Wnt/β-catenin signalling pathway on muscle development,[30] we cannot differentiate lower muscle mass of the $Slit3^{-/-}$ mice from muscle loss and from blunted growth development as an important limitation of our study. These should be further investigated.

In the present study, we found that treatment with the human SLIT3 LRRD2 for 4 weeks increased the relative muscle mass by 20.1% in the two mouse models. This efficacy is not satisfactory enough, especially compared to those of other agents currently under development.[36,37] However, the limited efficacy of SLIT3 LRRD2 may not be associated with its pharmacological properties but may be associated with its pharmacokinetic properties such as auto-antibody generation and rapid degradation *in vivo*.[5] Thus, the efficacy

of the human SLIT3 LRRD2 can be improved by using a strategy that minimizes auto-antibody generation and by developing a long-acting LRRD2 fragment by using drug-modification technologies. In fact, we observed that the half-life of SLIT3 LRRD2 *in vivo* was markedly short.

Here, we tested the therapeutic efficacy of SLIT3 LRRD2 *in vivo* using female OVX mice and aged male mice. Sham-operated and young mice were simultaneously examined to compare its efficacy, relatively. They represent two different pathophysiological mechanisms of muscle loss, thus our findings indicate that SLIT3 LRRD2 treatment is effective in muscle loss. However, the selection of middle-aged mice (18 month old) as an aging model could be considered as a limitation of this experiment. In addition, the SLIT3 LRRD2 treatment was effective in both male and female mice, and all muscular parameters were lower in both male and female $Slit3^{-/-}$ mice than in their WT littermates. These findings suggest that SLIT3 does not play any sex-specific roles in myogenesis.

ROBO2, a putative receptor for SLIT3, is ubiquitously expressed, raising an issue that SLIT3 LRRD2 treatment could cause off target effects. However, it is unlikely that the SLIT3 LRRD2 may act on brain because SLIT3 treatment did not cause any changes in the brain ultrastructure.[23] The kidney and the heart could potentially also be affected by SLIT3 LRRD2 treatment.[3,22] However, Xu *et al.*[23] reported that, even though SLIT3 treatment stimulated bone angiogenesis, it had no effects on vascular morphology of the kidney and the heart. Furthermore, in this study, the H&E staining and active β-catenin expression showed that SLIT3 LRRD2 treatment had no or negligible effect on the two organs. In addition, the gross examination of multiple organs and blood biochemistry testing were normal after the SLIT3 LRRD2 treatment in mice. Collectively, it is unlikely that SLIT3 LRRD2 treatment would cause off target effects in other organs, besides the muscles and the bone.

In conclusion, the results of the present study indicate that the SLIT3/ROBO system induces the myogenic differentiation of myoblasts through β-catenin signalling. Furthermore, our results suggest that SLIT3 LRRD2 can be developed as a novel therapeutic agent to reverse muscle loss.

Acknowledgements

Conflict of interest

Han Jin Cho, Young-Sun Lee, Seung Hun Lee, and Jung-Min Koh are inventors on the following patents: PCT/KR2017/005959

and PCT/KR2013/005282. Hyeonmok Kim, Sung Ah Moon, Jin-Man Kim, Hanjun Kim, Min Ji Kim, Jiyoung Yu, Kyunggon Kim, In-Jeoung Baek, Kyong Hoon Ahn, Sungsub Kim, and Jong-Sun Kang declare no competing financial interests.

Funding

Online supplementary material

Additional supporting information may be found online in the Supporting Information section at the end of the article.

Table S1. List of recombinant proteins and antibodies.
Table S2. Primer sequences used for semiquantitative RT-PCR.
Table S3. Primer sequences used for SYBR Green-based quantitative real-time PCR.
Table S4. Serum SLIT3 concentrations in ovariectomized mice with and without SLIT3 LRRD2 injections.
Table S5. Serum biochemical parameters in ovariectomized mice with and without SLIT3 LRRD2 injections.
Table S6. MRM transition table for LRRD2 quantitation.
Table S7. In vivo pharmacokinetics of LRRD2 in 9-week-old male C57BL/6 mice.
Table S8 Primer sequences and PCR conditions used for mouse genotyping.
Figure S1 Reduced skeletal muscle mass, strength, and physical activity in female Slit3$^{-/-}$ mice. (A) Slit3 mRNA expression in gastrocnemius muscle of 7-week-old female Slit3$^{-/-}$ mice and WT littermates (n = 3 per group) measured by real time PCR. 18S RNA was used as a loading control. (B) Body weight of 7-week-old female Slit3$^{-/-}$ mice and WT littermates (n = 10 per group). (C, D) The muscle mass of the mice was expressed as raw values (C), as well as the percentage of body weight (also referred to as relative muscle mass) (D). (E, F) Skeletal muscle strength and physical activity were determined based on the grip strength of the forelimbs and four paws (E) and daily wheel-running distance (F), respectively (n = 5 per group). *P < 0.05 compared to the WT littermates using the unpaired t-test.
Figure S2. Slit3 expression in calvaria and gastrocnemius muscle, and the effect of Slit3 overexpression on myoblast differentiation. (A) Slit3 expression in calvaria and gastrocnemius muscle of 16-week-old male C57BL/6 mice (n = 3/each)

measured by real time PCR. 18S RNA was used as a loading control. (B, C) C2C12 myoblasts were transfected with control and Slit3 expression vectors, and the expression of SLIT3 in the cell lysates and conditioned media (CM) was analysed by western blotting (B). Control and Slit3-transfected C2C12 myoblasts were differentiated for 3 or 4 days and myotubes were stained with the anti-myosin heavy chain antibody; the nuclei were counterstained with DAPI (C). The quantification of total myotube area is shown on the right. Scale bars: 200 μm. *P < 0.05 compared to the calvaria using the unpaired t-test. NS, not significant.
Figure S3. SLIT3 stimulates myogenin mRNA expression in myoblasts. (A) C2C12 myoblasts were incubated in the presence or absence of 1 μg/mL SLIT3 for 1 or 2 days. Cell viability was assessed using the CCK-8 assay. TNF-α (10 ng/mL) was used as a positive control. (B) C2C12 myoblasts were incubated with various concentrations of SLIT3 for 24 h. Cell proliferation was assessed by cell proliferation ELISA. (C) The C2C12 myoblasts were differentiated in the presence or absence of 1 μg/mL SLIT3 for 24 h, and real-time PCR was performed. The 18S rRNA gene was used as an internal control. Mrf4, myogenic regulatory factor 4; Myf5, myogenic factor 5; MyoD, myoblast differentiation protein 1; Mef, myocyte enhancer factor. *P < 0.05 compared with the untreated control cells using the unpaired t-test or Kruskal–Wallis test followed by Bonferroni correction. NS, not significant.
Figure S4. Activation of β-catenin signalling in various cell lines. (A) C2C12 myoblasts were treated with 1 μg/mL SLIT3 for the indicated times and western blotting was performed with their relevant antibodies. (B) C2C12 myoblasts, MC3T3-E1 osteoblasts, HepG2 hepatoma cells, and MCF-7 breast cancer cells were treated with 1 μg/mL SLIT3 for 2 h. Western blotting was performed to detect active (non-phosphorylated) and total β-catenin. Actin was used as an internal loading control for normalization. Quantification of western blotting results is shown in the lower panels. *P < 0.05 compared to the untreated control cells using the unpaired t-test.
Figure S5. Activation of β-catenin-associated signalling pathways by SLIT3. (A-C) C2C12 myoblasts were treated with 1 μg/mL SLIT3 for 24 h. (A) Western blotting was performed with an anti-nephrin antibody. GM and DM indicate growth and differentiation medium, respectively. Quantification of western blots is shown on the right. *P < 0.05 compared to the untreated control cells using the unpaired t-test. (B) Real-time PCR evaluating c-Myc expression. (C) AMP-activated protein kinase (AMPK) was evaluated by western blotting. (D) C2C12 myoblasts were treated with 1 μg/mL SLIT3 for the indicated time periods and protein levels of microtubule-associated protein 1-light chain 3B (LC3B) were determined by western blotting. Transforming growth factor-β1 (TGF-β1) was used as a positive control. Actin or 18S rRNA was used as internal loading controls. ND, not detected. NS, not significant.

Figure S6. Activation of β-catenin signalling by SLIT3 and Wnt3A. (A) C2C12 myoblasts were treated with 1 μg/mL SLIT3 and/or the indicated concentrations of Wnt3a conditioned media (CM) for 2 days. Myotubes were immunostained with the anti-myosin heavy chain antibody, and the nuclei were counterstained with DAPI. The quantification of total myotube area is shown on the right. *$P < 0.05$ compared to the untreated control using the Kruskal-Wallis test. Scale bars: 100 μm. NS, not significant. (B) C2C12 myoblasts were treated with 1 μg/mL SLIT3 or Wnt3a CM for 1 h. Ctrl = CM from the L929 control cells. Western blotting was performed to evaluate the components of canonical Wnt signalling. Actin was used as an internal loading control. Quantification of western blotting results is shown in the right and lower panels. *$P < 0.05$ compared to the untreated control or Ctrl CM-treated cells using the unpaired t-test. NS, not significant.

Figure S7. The effect of SLIT3 treatment on M-cadherin-associated complex. C2C12 myoblasts were treated with 1 μg/mL SLIT3 for the indicated times, and western blotting was performed after immunoprecipitation (IP) with M-cadherin. Actin was used as an internal loading control. Quantification of western blotting results is shown in the lower panels. *$P < 0.05$ compared to the untreated control using the Kruskal-Wallis test followed by Bonferroni correction.

Figure S8. Robo2 expression in major organs of 16-week-old male C57BL/6 mice (n = 3/organ) measured by real time PCR. 18S RNA was used as the loading control.

Figure S9 The effect of SLIT3 LRRD2 treatment on protein metabolism and muscular SLIT3 expression. (A) C2C12 myoblasts were treated with 10 nM SLIT3 LRRD2 for 30 min, and lysed after 30 min of incubation with 10 μM puromycin. Cell lysates were analysed by western blotting using an anti-puromycin antibody. IGF-1 was used as a positive control. Western blotting for protein synthesis-relating signalling molecules after the treatment with 10 nM SLIT3 LRRD2 for the indicated times was also shown in the right panel. (B) Protein degradation was performed in C2C12 myoblasts in the presence or absence of 10 nM SLIT3 LRRD2 for 9 h as described in the Supplemental Materials and Methods. TCA-soluble radioactivity released into the conditioned media was measured, and protein degradation was calculated. Western blotting for protein degradation-relating signalling molecules after the treatment with 10 nM SLIT3 LRRD2 for the indicated times was also shown in the right panel. (C) Western blotting

for protein metabolism-relating signalling molecules in gastrocnemius muscles of 7-week-old female Slit3$^{-/-}$ mice and WT littermates was shown. (D) Ovariectomized (OVX) C57BL/6 mice (n = 5 per group) were intravenously injected with PBS or 10 μg SLIT3 LRRD2 for 4 weeks. Sham operated mice (n = 4) were injected with PBS. The mice were sacrificed, and Slit3 expression in gastrocnemius muscle was measured by real time PCR. 18S RNA was used as the loading control. NS, not significant.

Figure S10. Effect of SLIT3 LRRD2 treatment on the heart and the kidney. (A) Nine-month-old male C57BL/6 mice (n = 6 per group) were intravenously injected with PBS or 45 μg SLIT3 LRRD2 for 4 weeks. The heart and the kidney were fixed in 4% paraformaldehyde and then stained with H&E. Representative images are shown. (B) Nine-month-old male C57BL/6 mice (n = 6 per group) were intravenously injected with PBS or 45 μg SLIT3 LRRD2 for 5 days. Immunohistochemical staining for active β-catenin of the organs was performed, based on 3,3′-diaminobenzidine staining. Arrows indicate nuclear β-catenin staining. Representative images and the quantification of β-catenin+ nuclei are shown in the left and right panels, respectively. *$P < 0.05$ compared to the untreated control mice using the unpaired t-test. Scale bars: 100 μm.

Figure S11 SLIT3 LRRD2 pharmacokinetics analysis. (A, B) Multiple reaction monitoring (MRM) peak of SLTSLVLYGNK peptide for LRRD2 pharmacokinetics analysis. (A) MRM peak from 5 transitions of light peptide of SLTSLVLYGNK were extracted using Skyline software. (B) MRM peak area of light peptide (red) and stable isotope-labelled internal standard (SIS) peptide (blue) from 10 time points (0.05, 0.12, 0.25, 0.05, 1, 2, 4, 6, 8, 24 h) after the LRRD2 treatment in mice. SIS peptide was spiked into each sample at 500 fmol to serve as an internal standard. (C) Concentration-time profiles of LRRD2 in 8-week-old ovariectomized C57BL/6 mice (n = 4 per group) intravenously injected with PBS or 2.25 mg/kg SLIT3 LRRD2. The levels from the MRM analysis were plotted as the time profile with standard deviation at each time point. Concentration after the 8 h time point was omitted. Concentrations above and below lower limit of quantitation (LLOQ) were shown as black-filled squares with blue line and grey-filled squares with blue line, respectively.

Figure S12 A proposed mechanism of SLIT3-induced myoblast differentiation.

References

1. Cruz-Jentoft AJ, Bahat G, Bauer J, Boirie Y, Bruyère O, Cederholm T, et al. Sarcopenia: revised European consensus on definition and diagnosis. *Age Ageing* 2019;**48**:16–31.
2. Kwak JY, Kwon K-S. Pharmacological interventions for treatment of sarcopenia: current status of drug development for sarcopenia. *Ann Geriatr Med Res* 2019;**23**:98–104.
3. Grieshammer U, Le M, Plump AS, Wang F, Tessier-Lavigne M, Martin GR. SLIT2-mediated ROBO2 signaling restricts kidney induction to a single site. *Dev Cell* 2004;**6**:709–717.
4. Macias H, Moran A, Samara Y, Moreno M, Compton JE, Harburg G, et al. SLIT/ROBO1 signaling suppresses mammary branching morphogenesis by limiting basal cell number. *Dev Cell* 2011;**20**:827–840.
5. Kim BJ, Lee YS, Lee SY, Baek WY, Choi YJ, Moon SA, et al. Osteoclast-secreted SLIT3

coordinates bone resorption and formation. *J Clin Invest* 2018;**128**:1429–1441.

6. Hirschfeld HP, Kinsella R, Duque G. Osteosarcopenia: where bone, muscle, and fat collide. *Osteoporos Int* 2017;**28**:2781–2790.

7. Sundaresan V, Roberts I, Bateman A, Bankier A, Sheppard M, Hobbs C, et al. The DUTT1 gene, a novel NCAM family member is expressed in developing murine neural tissues and has an unusually broad pattern of expression. *Mol Cell Neurosci* 1998;**11**:29–35.

8. Halperin-Barlev O, Kalcheim C. Sclerotome-derived Slit1 drives directional migration and differentiation of Robo2-expressing pioneer myoblasts. *Development* 2011;**138**:2935–2945.

9. Yuan W, Rao Y, Babiuk RP, Greer JJ, Wu JY, Ornitz DM. A genetic model for a central (septum transversum) congenital diaphragmatic hernia in mice lacking Slit3. *Proc Natl Acad Sci U S A* 2003;**100**:5217–5222.

10. Edström E, Ulfhake B. Sarcopenia is not due to lack of regenerative drive in senescent skeletal muscle. *Aging Cell* 2005;**4**:65–77.

11. Deacon RM. Measuring the strength of mice. *J Vis Exp* 2013.

12. Zammit PS. Function of the myogenic regulatory factors Myf5, MyoD, Myogenin and MRF4 in skeletal muscle, satellite cells and regenerative myogenesis. *Semin Cell Dev Biol* 2017;**72**:19–32.

13. Rhee J, Buchan T, Zukerberg L, Lilien J, Balsamo J. Cables links Robo-bound Abl kinase to N-cadherin-bound beta-catenin to mediate Slit-induced modulation of adhesion and transcription. *Nat Cell Biol* 2007;**9**:883–892.

14. Prasad A, Paruchuri V, Preet A, Latif F, Ganju RK. Slit-2 induces a tumor-suppressive effect by regulating beta-catenin in breast cancer cells. *J Biol Chem* 2008;**283**:26624–26633.

15. Suzuki A, Pelikan RC, Iwata J. WNT/beta-catenin signaling regulates multiple steps of myogenesis by regulating step-specific targets. *Mol Cell Biol* 2015;**35**:1763–1776.

16. Rodriguez J, Vernus B, Chelh I, Cassar-Malek I, Gabillard JC, Hadj Sassi A, et al. Myostatin and the skeletal muscle atrophy and hypertrophy signaling pathways. *Cell Mol Life Sci* 2014;**71**:4361–4371.

17. Tseng RC, Lee SH, Hsu HS, Chen BH, Tsai WC, Tzao C, et al. SLIT2 attenuation during lung cancer progression deregulates beta-catenin and E-cadherin and associates with poor prognosis. *Cancer Res* 2010;**70**:543–551.

18. Stein E, Tessier-Lavigne M. Hierarchical organization of guidance receptors: silencing of netrin attraction by slit through a Robo/DCC receptor complex. *Science* 2001;**291**:1928–1938.

19. Morlot C, Hemrika W, Romijn RA, Gros P, Cusack S, McCarthy AA. Production of Slit2 LRR domains in mammalian cells for structural studies and the structure of human Slit2 domain 3. *Acta Crystallogr D Biol Crystallogr* 2007;**63**:961–968.

20. Chen JH, Wen L, Dupuis S, Wu JY, Rao Y. The N-terminal leucine-rich regions in Slit are sufficient to repel olfactory bulb axons and subventricular zone neurons. *J Neurosci* 2001;**21**:1548–1556.

21. Howitt JA, Clout NJ, Hohenester E. Binding site for Robo receptors revealed by dissection of the leucine-rich repeat region of Slit. *EMBO J* 2004;**23**:4406–4412.

22. Qian L, Liu J, Bodmer R. Slit and Robo control cardiac cell polarity and morphogenesis. *Curr Biol* 2005;**15**:2271–2278.

23. Xu R, Yallowitz A, Qin A, Wu Z, Shin DY, Kim JM, et al. Targeting skeletal endothelium to ameliorate bone loss. *Nat Med* 2018;**24**:823–833.

24. Blockus H, Chédotal A. Slit-Robo signaling. *Development* 2016;**143**:3037–3044.

25. Knight JD, Kothary R. The myogenic kinome: protein kinases critical to mammalian skeletal myogenesis. *Skelet Muscle* 2011;**1**:29.

26. von Maltzahn J, Chang NC, Bentzinger CF, Rudnicki MA. Wnt signaling in myogenesis. *Trends Cell Biol* 2012;**22**:602–609.

27. Polesskaya A, Seale P, Rudnicki MA. Wnt signaling induces the myogenic specification of resident CD45+ adult stem cells during muscle regeneration. *Cell* 2003;**113**:841–852.

28. Rochat A, Fernandez A, Vandromme M, Moles JP, Bouschet T, Carnac G, et al. Insulin and wnt1 pathways cooperate to induce reserve cell activation in differentiation and myotube hypertrophy. *Mol Biol Cell* 2004;**15**:4544–4555.

29. Han XH, Jin YR, Seto M, Yoon JK. A WNT/beta-catenin signaling activator, R-spondin, plays positive regulatory roles during skeletal myogenesis. *J Biol Chem* 2011;**286**:10649–10659.

30. Bernardi H, Gay S, Fedon Y, Vernus B, Bonnieu A, Bacou F. Wnt4 activates the canonical beta-catenin pathway and regulates negatively myostatin: functional implication in myogenesis. *Am J Physiol Cell Physiol* 2011;**300**:C1122–C1138.

31. Jones AE, Price FD, Le Grand F, Soleimani VD, Dick SA, Megeney LA, et al. Wnt/beta-catenin controls follistatin signalling to regulate satellite cell myogenic potential. *Skelet Muscle* 2015;**5**:14.

32. Pan YC, Wang XW, Teng HF, Wu YJ, Chang HC, Chen SL. Wnt3a signal pathways activate MyoD expression by targeting cis-elements inside and outside its distal enhancer. *Biosci Rep* 2015;**35**.

33. Perry RL, Rudnick MA. Molecular mechanisms regulating myogenic determination and differentiation. *Front Biosci* 2000;**5**:D750–D767.

34. Suzuki A, Minamide R, Iwata J. WNT/beta-catenin signaling plays a crucial role in myoblast fusion through regulation of nephrin expression during development. *Development* 2018;**145**.

35. Sohn RL, Huang P, Kawahara G, Mitchell M, Guyon J, Kalluri R, et al. A role for nephrin, a renal protein, in vertebrate skeletal muscle cell fusion. *Proc Natl Acad Sci U S A* 2009;**106**:9274–9279.

36. Morvan F, Rondeau JM, Zou C, Minetti G, Scheufler C, Scharenberg M, et al. Blockade of activin type II receptors with a dual anti-ActRIIA/IIB antibody is critical to promote maximal skeletal muscle hypertrophy. *Proc Natl Acad Sci U S A* 2017;**114**:12448–12453.

37. Lach-Trifilieff E, Minetti GC, Sheppard K, Ibebunjo C, Feige JN, Hartmann S, et al. An antibody blocking activin type II receptors induces strong skeletal muscle hypertrophy and protects from atrophy. *Mol Cell Biol* 2014;**34**:606–618.

38. von Haehling S, Morley JE, Coats AJS, Anker SD. Ethical guidelines for publishing in the *Journal of Cachexia, Sarcopenia and Muscle*: update 2019. *J Cachexia Sarcopenia Muscle* 2019;**10**:1143–1145.